Fluorescence Assay for Neurotoxin-Modulated Ion Transport by the Reconstituted Voltage-Activated Sodium Channel Isolated from Eel Electric Organ†

Sally A. Tomiko, Robert L. Rosenberg, Mark C. Emerick, and William S. Agnew*
Department of Physiology, Yale University School of Medicine, New Haven, Connecticut 06510
Received August 19, 1985

ABSTRACT: A fluorescence assay for measuring Na channel activation in liposomes containing voltage-sensitive Na channels isolated from *Electrophorus electricus* is described. The assay is based on transport of a heavy-metal cation, Tl^+, through the activated channel to quench fluorescence of an internalized, water-soluble chromophore. The channel is "locked" in a chronically opened configuration with alkaloid neurotoxins such as veratridine or batrachotoxin. Diffusion potentials are used to amplify the signal, and enlarged liposomes (>8000 Å) result in time courses extended to the range of seconds. Analysis of the kinetics of quenching yields parameters that behave as linear functions of channel activation and reflect vesicle size and channel abundance. The $k_{1/2}$'s for activation by veratridine and batrachotoxin were 5 μM and 169 nM, respectively, and that for tetrodotoxin blockade was 4 nM. Externally applied QX-222 and tetrodotoxin each acted to partially block the stimulated signal, as expected for compounds that act on oppositely oriented channels in the membrane. Single-channel conductances estimated with either veratridine or batrachotoxin ranged between 0.6 and 40.7 pS, corresponding to transport numbers of (1.2×10^5) to (8.1×10^6) ions s^{-1} $channel^{-1}$ under the conditions of assay. The assay is approximately 100-fold more sensitive than radiotracer influx assays, requiring 1 fmol of protein per time course.

Voltage-sensitive Na channels, responsible for the initial depolarization of the action potential, are complex integral membrane proteins of approximately 300 000 daltons [for review, see Agnew (1984)]. The channels form rapidly conducting ion-selective pores through the membrane when activated by changes in membrane voltage or when modified by the binding of certain specific neurotoxins [for review, see Cahalan (1980)]. Na channels were first isolated as the tetrodotoxin (TTX)[1] and saxitoxin (STX) receptors from eel electric organ (Agnew et al., 1978; Miller et al., 1983), mammalian muscle (Barchi et al., 1980), mammalian brain (Hartshorne & Catterall, 1981, 1984), and other tissues (Villegas et al., 1983; Lombet & Lazdunski, 1984). When these proteins were reincorporated into lipid vesicles, Na^+ transport could be demonstrated upon addition of activating neurotoxins (Weigele & Barchi, 1982; Tanaka et al., 1983; Talvenheimo et al., 1982; Tamkun et al., 1984; Rosenberg et al., 1984a). Neurotoxins have also been used to remove inactivation and allow measurements of the activity of reconstituted channels incorporated into planar bilayers. Channels purified from rat brain, introduced into planar bilayers and treated with batrachotoxin (Hartshorne et al., 1985), behaved in a manner very similar to batrachotoxin-treated channels derived from native synaptosomal membranes in earlier studies (Krueger et al., 1983). Activity attributed to purified rat brain Na channels in planar bilayers, in the absence of toxins, has also been reported by Hanke et al. (1984). Normal biophysical properties in the absence of neurotoxins have been observed with the purified, reconstituted channel from eel with patch-clamp recording techniques (Rosenberg et al., 1984b). These properties included voltage-dependent activation, inactivation, single-channel conductance, mean channel open time, and ion selectivity quite similar to those for channels in native membranes of other cell types. Collectively, these findings demonstrate the feasibility of preparing artificial membranes that exhibit Na currents characteristic of nerve and muscle cells.

To facilitate studies of mechanisms of gating, transport, and drug action, it is important to optimize biochemical measurements of channel function. Until now, biochemical assays have been limited to tracer studies conducted with radioisotopes, such as $^{22}Na^+$. In these procedures, vesicle suspensions are treated with activating or blocking neurotoxins and then mixed with trace levels of the isotope. At intervals of several seconds, the internalized tracer is separated from the external label by eluting the mixture through small ion-exchange columns. In quench-flow experiments, Tanaka et al. (1983) extended the time resolution of this approach to <0.1 s. Limitations of these assays are that they are slow to execute, yield a limited number of data points, and in general require comparatively large amounts of protein.

We describe here a fluorescence assay for neurotoxin-activated transport by the reconstituted Na channel from eel electroplax. [Preliminary results have been published elsewhere; Tomiko et al. (1984).] The assay employs three strategies. First, by adaptation of a technique used with native and reconstituted nicotinic acetylcholine receptors (Moore & Raftery, 1980; Wu et al., 1981), the transport of a heavy-metal cation, Tl^+, through the neurotoxin-activated channel is reported by the collisional quenching of a highly fluorescent water soluble chromophore trapped in the vesicle interior. Second, to amplify the signal and to improve the signal-to-noise ratio, diffusion potentials are used (Talvenheimo et al., 1982; Garty et al., 1983) to selectively concentrate Tl^+ in nonleaky

† Supported by National Institutes of Health Grant NS17928 and a grant from the Multiple Sclerosis Society. S.A.T. is supported by a postdoctoral fellowship from the Muscular Dystrophy Association.
* Author to whom correspondence should be addressed.

[1] Abbreviations: PE, phosphatidylethanolamine; PS, phosphatidylserine; PC, phosphatidylcholine; ANTS, 8-aminonaphthalene-1,3,6-trisulfonate; TTX, tetrodotoxin; STX, saxitoxin; VTN, veratridine; BTX, batrachotoxin; FTS, freeze–thaw–sonication; EGTA, ethylene glycol bis(β-aminoethyl ether)-*N*,*N*,*N*′,*N*′-tetraacetic acid; HEPES, *N*-(2-hydroxyethyl)piperazine-*N*′-2-ethanesulfonic acid; BSA, bovine serum albumin; Tris, tris(hydroxymethyl)aminomethane.

0006-2960/86/0425-2162$01.50/0

vesicles containing activated channels. Third, Tl^+ influx kinetics are slowed by creating extremely large vesicles. Small liposomes formed initially during reconstitution are expanded in a freeze–thaw–sonication cycle. With an appropriate mixture of phospholipids, vesicles of large internal volume are produced, extending the equilibration time course from the range of milliseconds to seconds. This makes it possible to measure the continuous quench reaction in the quartz cell of a flow fluorometer connected to a sample mixing assembly. This procedure is sensitive, reproducible, and convenient to perform. The kinetics of the fluorescence signal are described by an uncomplicated transport theory that lends itself to physical interpretation. Analysis of the quench kinetics yields parameters reflecting channel activation, surface abundance, and vesicle size. We expect the assay to be a valuable tool in our efforts to monitor the functional effects of specific toxin binding and chemical modification of the protein structure.

Materials and Methods

Materials. Phosphatidylethanolamine (PE, prepared by enzymatic transphosphatidylation of egg yolk PC), phosphatidylserine (PS, from bovine brain), and phosphatidylcholine (PC, from fresh egg yolks) were from Avanti Biochemicals, Birmingham, AL. Bio-Beads SM-2 were from Bio-Rad. $^{22}NaCl$ was from Amersham (~1 mCi/mL, carrier free). $TlNO_3$ was from Fluka AG. Na_2H-ANTS (8-aminonaphthalene-1,3,6-trisulfonate) was from TCI-C.P. Veratridine (VTN, from Aldrich) was prepared as a 2 mM suspension in isosmolar Tris-SO_4 (pH 7.4) by brief sonication. Batrachotoxin (BTX, generous gift of Dr. John Daly, National Institutes of Health) was dissolved to 500 μM in ethanol and stored at −20 °C in 100-μL aliquots. Dibucaine was from ICN Pharmaceuticals. QX-222 from Astra Pharmaceutical was the gift of Dr. R. Aldrich. All other reagents were from Sigma Chemical Co.

Purification of TTX-Binding Protein. Purification procedures were as described by Rosenberg et al. (1984a,b). The purified sample (100–150 μg of protein/mL and 800–1000 pmol of [^{3}H]TTX binding sites/mg of protein) pooled from the Sepharose 6B column was dialyzed to substitute sulfate anions for phosphate anions. Dialysis was for 3 h at 0 °C with three changes of ~100 volumes. The dialysis solution was either 84 mM Na_2SO_4, 1 mM EGTA, and 10 mM HEPES–NaOH, pH 7.4, or 13.5 mM Na_2SO_4, 163 mM Tris-SO_4, and 1 mM EGTA, pH 7.4. The osmolarity of these solutions averaged 220 mOsm/kg, measured by a Wescor 5100C vapor-pressure osmometer.

Reconstitution. Sonicated liposomes of PE/PS/PC (5:4:1 molar ratio, 40 mg/mL) were added to a dialyzed sample to yield a final concentration of 10 mg of lipid/mL. Bio-Beads were then added to 0.3 g/mL, and the sample was agitated for 5 h at 4 °C, filtered, and stored at 0 °C. Aliquots were subjected to freeze–thaw–sonication (FTS; Rosenberg et al., 1984a) before each experiment to create larger vesicles. After this step, all solutions that came in contact with the vesicles were osmotically adjusted.

Column Preparation. Dowex 50X-80–100 was used to remove external Na^+ from samples in exchange for $Tris^+$. Columns of Dowex prepared in isosmolar sucrose plus 3.3 mg of bovine serum albumin (BSA) per milliliter were poured in small Pasteur pipets and used to bind external $^{22}Na^+$ in the radiotracer flux assay (Gasko et al., 1976; Rosenberg et al., 1984a). Dowex columns were also used to generate diffusion potentials before beginning radiotracer or fluorescence quench assays (Garty et al., 1983). These were rinsed with isosmolar Tris-SO_4 plus 3.3 mg of BSA per milliliter and stored at room temperature for up to 8 h before use. Each column was used up to 4 times (the capacity for Na^+ is 2.0 mequiv/mL of wet resin).

Radiotracer Assays. These were performed as described by Rosenberg et al. (1984a). In some instances, however, FTS vesicles (200 μL) were eluted through Dowex columns with isosmolar Tris-SO_4 (≥1.2 mL) to generate a diffusion potential before addition of $^{22}Na^+$ to 10 μCi/mL.

Equipment for Fluorescence Assay. Fluorescence was monitored with an FS950 Fluoromat (Kratos Analytical Instruments) fitted with a standard 28-μL quartz flow cell, illuminated volume = 20 μL. Use of a blue-filtered excitation lamp with peak at 365 nm, a 365-nm band excitation filter, and a 470-nm cutoff emission filter provided optimal conditions for detecting ANTS fluorescence, while excluding wavelengths that either harm Na channels (~280 nm; Fox, 1974) or elicit Tl^+ fluorescence (excitation ~214 nm, emission 310–450 nm; Udenfriend, 1962). Fluorescence output was monitored on a multimeter (Fluka, 8062A True RMS) in parallel with a variable speed chart recorder. Teflon tubing (0.3-mm i.d.) led from the flow cell back to two 1-mL disposable tuberculin syringes by way of a glass capillary Y connector. Glass bead irregularities annealed to the internal surface of this connector served to create turbulence. Tygon tubing (1-mm i.d.) interconnected the Y connector to both the Teflon tubing and two 16-gauge needles. For sample application, syringes were attached to the needles and held in place by two stationary clamps. A grooved rigid bar placed over the syringe plungers was pushed for isovolumetric delivery of the solutions; this resulted in a "dead time" after mixing of ~2 s. Time courses were monitored from the time flow was stopped.

Sample Preparation. Na_2H-ANTS was prepared as a 120 mM stock solution in 174 mM Tris-SO_4, pH-adjusted to 7.4 with NaOH, and stored in the dark. ANTS (3 or 30 mM) was internalized during vesicle formation by FTS. Sonication was generally limited to 2 s because of the small sample volumes (260 μL). External ANTS was removed by centrifugation of samples through Sephadex G-50 (Levinson et al., 1979). The Sephadex G-50 was preequilibrated with Na_2SO_4 in 10 mM HEPES at Na^+ concentration and osmolarity equal to that of the ANTS/vesicle solution (osmolarity maintained with Tris-SO_4). This gel filtration removed more than 99.9% of the external ANTS with recovery of more than 94% of the vesicles. The sample was then diluted to 2–5 mL and kept on ice. $TlNO_3$ (or $NaNO_3$) solutions of twice the desired final concentration were prepared in either isosmolar Na_2SO_4/10 mM HEPES or Tris-SO_4.

Experimental Protocols. Pretreatment with inhibitory drugs or toxins was for 12 min at 0 °C. Subsequent incubation with or without VTN was for 6 min at 30 °C; incubation with or without BTX was for 36 min at 30 °C. After toxin incubation, 200 μL of sample was applied to a Dowex column and rinsed with 1.2 mL of isosmolar Tris-SO_4 to remove external Na^+. In some experiments, the sample was diluted with isosmolar Na_2SO_4/HEPES solution. A 0.6-mL aliquot, supplemented with toxin(s), was drawn into the sample syringe and connected to the assay system. The other syringe contained the appropriate $TlNO_3$ (or $NaNO_3$) solution. Three 1-min time courses were recorded, each reflecting the activity of 1–10 fmol of Na channel (based on [^{3}H]TTX binding activity). Time between samples could be reduced to 6 min to permit as many as 10 triplicate assays/h.

Data Analysis. Replicate time courses were averaged, and changes in fluorescence at various times after $t = 0$ were measured. These changes in fluorescence in the presence or

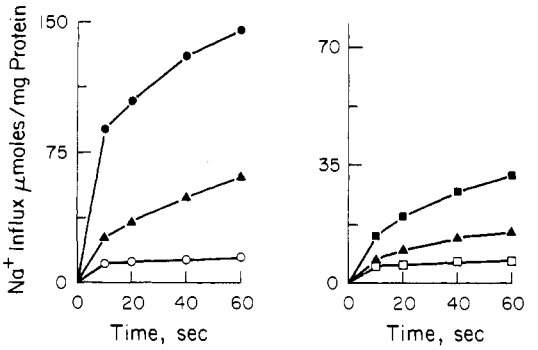

FIGURE 1: Neurotoxin-stimulated $^{22}Na^+$ uptake. Purified Na channel samples were preequilibrated in 84 mM Na_2SO_4, 1 mM EGTA, and 10 mM HEPES–NaOH, pH 7.4, before addition of exogenous lipid and removal of detergent to yield reconstituted vesicles. (Left panel) Vesicles were treated with (●) 5 μM BTX in ethanol (1% final, v/v), (▲) 5 μM BTX + 1 μM TTX external, or (○) ethanol vehicle alone (1% final, v/v), and influx was measured as described by Rosenberg et al. (1984a) (n = 1). (Right panel) Vesicles were treated with (■) 100 μM veratridine, (▲) 100 μM veratridine + 1 μM TTX external, or (□) the veratridine vehicle alone (175 mM Tris-SO_4, pH 7.4), and influx was measured (n = 1).

absence of toxin could be compared as the ratio of the two values or the difference between them. Graphical analysis of the quench kinetics, as described under Results and Discussion and the Mathematical Appendix, was carried out manually or with a NorthStar Horizon computer. For such analysis, the fluorescence curves were scaled so that fluorescence at t = 0, F_0, was set equal to 1, and a reference fluorescence was chosen and set equal to 0. Fluorescence at infinite time, F_∞, was then some fraction of 1.

Results and Discussion

Toxin-Modified Radiotracer Influx. The standard for comparison during development of this fluorescence assay for Na channel activity in reconstituted vesicles was our previous results with the radiotracer assay (Rosenberg et al., 1984a,b). The assay must reproducibly provide information of the sort obtained from $^{22}Na^+$ uptake studies and illustrated in Figure 1. Here, the reconstituted channel was activated with BTX (left panel, 5 μM) or VTN (right panel, 100 μM). Controls with the toxin vehicles alone showed low background influx. BTX stimulated flux by about 9-fold above control and VTN by about 4-fold. In each instance 1 μM external TTX blocked toxin-stimulated influx by about 70%. Initial toxin-stimulated influx rates were ~460 μmol of Na^+ (mg of protein)$^{-1}$ min^{-1} with BTX and ~55 μmol of Na^+ (mg of protein)$^{-1}$ min^{-1} with VTN.

Tl^+ Quenching of ANTS Fluorescence. ANTS has a number of properties making it well suited for this assay; it does not adsorb to liposomes, and when trapped internally during FTS, the dye's charges prevent it from leaking into solution [cf. Moore & Raftery (1980)]. The intense fluorescence made the dye easy to detect in vesicles containing <0.05% of the total sample volume. At solution concentrations below 0.15 mM the excitation maximum was 370 nm and the emission maximum was 515 nm; at higher concentrations (>0.17 mM), there was a progressive shift of the apparent excitation maximum (to ~440 nm at 25 mM). This effect, which may result from self-absorption, was not seen even at much higher intravesicular concentrations when vesicles were in dilute suspension. Most importantly, ANTS fluorescence is quenched by Tl^+, which can pass through Na channels (Hille, 1972; Khodorov, 1978), and can thus serve as a reporter of channel activity. Tl^+ quenched ANTS fluorescence in a concentration-dependent manner that was independent of the

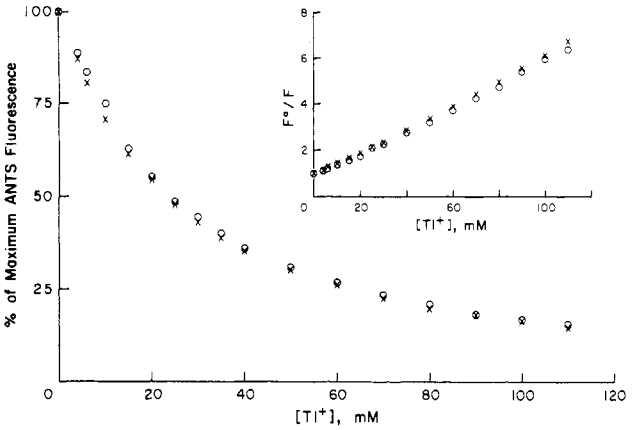

FIGURE 2: Tl^+ quench of ANTS fluorescence (×) in solution and (○) internalized in vesicles is equivalent. (×) Fluorescence of 12 mM Na_2H-ANTS (pH 7.4 in 8 mM Na_2SO_4) was measured in the presence of increasing concentrations of $TlNO_3$. Ionic strength was held constant by substituting $TlNO_3$ for $NaNO_3$ in solutions buffered with 10 mM HEPES, pH 7.4. K_s = 51.8 M^{-1}. (○) Reconstituted vesicles were equilibrated with 30 mM ANTS (pH 7.4) during FTS, and external ANTS was removed by gel filtration. Each sample was diluted in appropriate $TlNO_3/NaNO_3$ solution; overall ANTS concentration was 9 μM (i.e., intravesicular volume was 6 nL or 0.03% of the suspension). Fluorescence was measured 21 h later. K_s = 49.7 M^{-1}. (Inset) Data plotted according to eq 1. Slope of line = Stern–Volmer constant (K_s).

dye concentration (Figure 2). The data were linearized by replotting (Figure 2, inset) according to the Stern–Volmer relation for collisional quenching [see Eftink & Ghiron (1981)]

$$F^0/F = 1 + K_s[Tl^+] \quad (1)$$

where F^0 is the unquenched fluorescence and F is the quenched signal. K_s is the Stern–Volmer quenching constant equal to the reciprocal of the Tl^+ concentration producing a 50% decrease in fluorescence. Quenching is illustrated for 12 mM ANTS in free solution and for 30 mM ANTS trapped inside a vesicle preparation (9 μM overall concentration) that was fully equilibrated with various concentrations of $TlNO_3$. The K_s's for vesiculated (49.7 M^{-1}) and nonvesiculated (51.8 M^{-1}) ANTS were nearly identical. Thus, fluorescence accurately reported the Tl^+ concentration in the vesicle interior, and the signal was reduced 50% by 20 mM Tl^+.

Channel-Facilitated Entry of Tl^+. Thallous ion (added as NO_3^- salt) enters FTS vesicles over many seconds, as expected from its relatively low lipid permeability (Gutknecht, 1983). Figure 3 illustrates traces obtained with the fluorometer apparatus described under Materials and Methods. Duplicate recordings in (a) show no effect on fluorescence when ANTS-loaded, reconstituted vesicles were rapidly mixed with $NaNO_3$. However, some quenching was observed when $TlNO_3$ was used in the absence of activating neurotoxins (b). This quenching was markedly accelerated when the vesicles were pretreated with BTX (c). That this stimulation was due to activation of Na channels was shown by the absence of a BTX effect when vesicles were preequilibrated with 1 μM TTX inside and outside (d vs. e).

Absence of Toxic Effects of Thallous Ion on the Na Channel. The utility of this assay hinges on the ability of Tl^+ to substitute for $^{22}Na^+$ without damaging the channel behavior. Hille (1972) has reported that Tl^+ directly inactivates Na channels in frog sciatic nerve preparations. A series of control experiments have indicated that the reconstituted channel was not adversely affected by even extended exposure to high concentrations of thallous ion. For example, in one study, vesicle suspensions were incubated with solutions of $TlNO_3$

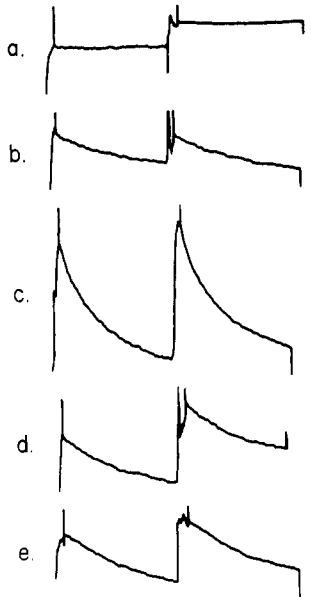

FIGURE 3: Quench of vesiculated ANTS fluorescence by Tl^+ reflects the conductance state of the Na channel. Vesicles, as in Figure 1 but containing 3 mM ANTS, were applied to Dowex 50 columns and eluted with isosmolar Tris-SO_4 to strip external Na^+ in exchange for $Tris^+$ before assay. Each panel consists of duplicate 1-min time courses of fluorescence after mixing vesicles with isosmolar cation solution. Vertical event marker indicated cessation of sample delivery and initiation of time course. (a) Vesicles were incubated in 2.5 μM BTX and mixed with 50 mM $NaNO_3$. Different preparations of vesicles were treated with (b) 1% ethanol vehicle alone or (c) 5 μM BTX and mixed with 80 mM $TlNO_3$. A third batch of vesicles was equilibrated with 1 μM TTX during FTS and treated with (d) 1% ethanol or (e) 5 μM BTX before mixing with 80 mM $TlNO_3$.

of 0, 20, 60, and 100 mM for 3 min or 1 h, followed by exchange of external cations for $Tris^+$ to create a diffusion potential (cf. Materials and Methods). The $^{22}Na^+$ uptake stimulated by BTX was then monitored in standard tracer influx assays. Neither the brief nor more extended exposure to Tl^+ at any concentration reduced the fold stimulation by BTX. There was a small decrease in the rate of uptake in both controls and BTX-stimulated fluxes at progressively higher concentrations of Tl^+ (14% after 3-min exposure to 100 mM $TlNO_3$ and 37% after 1 h). In other experiments, the stability of the solubilized [^{3}H]TTX binding site was tested in the presence of $TlNO_3$ with a thermal inactivation protocol based on the observations of Agnew and Raftery (1979). A solubilized extract was made labile by incubating at 22 °C after raising the detergent concentration to 2.5% (w/v) to reduce the ratio of lipid to detergent. The first-order rate of denaturation was measured in the presence of 0, 20, 60, and 100 mM $TlNO_3$. The rate constants [k_r; cf. Agnew & Raftery (1979)] were 0.050, 0.055, 0.058, and 0.071 min^{-1}. These correspond to a net effect on denaturation over the course of a 3-min incubation of no more than 5%; with respect to toxin binding, the protein was insignificantly affected by Tl^+.

Thus, whereas Hille (1972) found Na currents to be lost within 1 min of exposure to the Tl^+ salts, we have not yet encountered any behavior indicating that the channel is rapidly destroyed or modified by Tl^+. The differences between these observations might reflect that our studies have been conducted in defined buffer solutions, thereby avoiding microprecipitates (such as TlCl) that might form in axoplasm, or that these studies have employed neurotoxins as channel activators.

Enhancement of Toxin-Stimulated Signals by Diffusion Potentials. Although transport through the channel is passive, permeant cations may be concentrated above their external

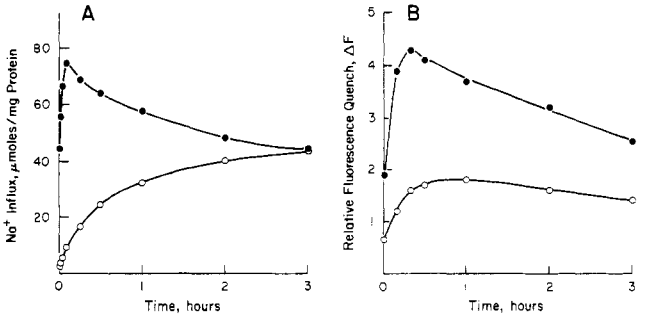

FIGURE 4: BTX-stimulated $^{22}Na^+$ influx and fluorescence quench attain transient maxima in the presence of diffusion potential. (A) Vesicles prepared in Na_2SO_4 solution as in Figure 1 were treated with (●) 5 μM BTX or (○) ethanol vehicle alone. Each sample was applied to a Dowex 50 column and eluted with isosmolar Tris-SO_4 to strip external Na^+ in exchange for $Tris^+$. Samples were supplemented with BTX (to 5 μM) or vehicle and with Na_2SO_4 to 8.4 mM final concentration ($[Na^+]_{in}/[Na^+]_{out} = 10$). Assay was initiated by addition of $^{22}Na^+$ (10 μCi/mL) and influx measured at the times indicated. (B) Vesicles (preequilibrated in 13.5 mM Na_2SO_4, 163 mM Tris-SO_4, and 1 mM EGTA, pH 7.4) containing 3 mM ANTS (so $[Na^+_i] \sim 40$ mM) were incubated in (●) 5 μM BTX or (○) ethanol vehicle. After elution through Dowex, samples were mixed with isosmolar Tris-SO_4 containing 8 mM $TlNO_3$ so that $[Na_+]_{in}/[Tl^+]_{out} \sim 10$. Aliquots were withdrawn, and fluorescence was measured at the times indicated. The decline in fluorescence relative to $t = 0$ is plotted on the ordinate.

levels by creating diffusion potentials and exploiting the channel's cation selectivity. Reducing $[Na^+_o]$ relative to $[Na^+_i]$ initially results in net Na^+ efflux. However, if other internal and external ions are impermeant, the loss of net positive charge produces a diffusion potential that impedes further Na^+ efflux. Thereafter, Na^+ will exit the vesicle only in exchange for an external permeant cation, which can thereby be concentrated to levels approaching the initial $[Na^+_i]$. Leaky vesicles should not exhibit cation-selective electroneutral exchange and should merely equilibrate with the external solution.

Diffusion potentials were created in the standard radiotracer assay by diluting the reconstituted vesicles 4-fold into Tris-SO_4 solution containing trace $^{22}Na^+$ (Rosenberg et al., 1984a). If, instead, external Na^+ is completely removed by ion exchange (Garty et al., 1983), Na^+ can be then added back to create specifically desired ratios of $[Na^+_i]/[Na^+_o]$. Figure 4A illustrates the time course of $^{22}Na^+$ uptake after ion exchange when the $[Na^+_i]/[Na^+_o]$ was set to 10. The influx of $^{22}Na^+$ in the presence of 5 μM BTX rose sharply above its equilibrium value for 5 min before beginning a slow decline. A much slower rate of influx was observed in the absence of toxin. Stimulation by BTX over the control was 17-fold at 30 s, declining to 8-fold by 5 min. The declining phase of the stimulated influx reflects dissipation of the diffusion potential, in part due to the leak of internal anions from the vesicle interior. Substituting sulfate for phosphate as the internal anion reduced this leak so that toxin-stimulated signals were increased and the duration of the diffusion potential was prolonged. For routine measurements, assays were conducted only during the first minute, before rundown became significant.

Figure 4B illustrates an analogous "overshoot" experiment carried out with the fluorescence assay. Vesicles treated with 5 μM BTX transiently loaded Tl^+ above the external concentration of 4 mM, producing an amplified quench signal that began to decline after 20 min. In other experiments the peak occurred at 5–30 min ($n = 5$). Some portion of the leak also reflects cation-selective vesicles responding weakly to the diffusion potential; the quenching in the controls was amplified

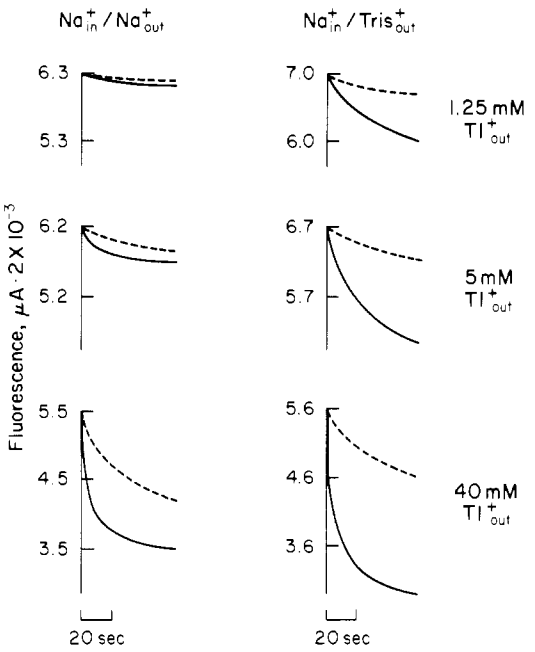

FIGURE 5: Amplification of alkaloid-stimulated quench by diffusion potential. Vesicles containing 30 mM ANTS were incubated in 5 μM BTX in ethanol (solid lines) or ethanol alone (dashed lines) for 36 min at 30 °C. Fluorescence of vesiculated ANTS was measured during 1 min in 1.25, 5.0, or 40 mM $TlNO_3$. (Left column) Before assay, samples were diluted into six parts of isosmolar Na_2SO_4/10 mM HEPES, pH 7.4. (Right column) Before assay, samples were applied to Dowex columns and rinsed with six parts of isosmolar Tris-SO_4, pH 7.4, to strip external Na^+ in exchange for $Tris^+$.

with slower kinetics and to a much lesser extent. In these "overshoot" experiments, care was taken to avoid Tl^+ precipitation. The combination of $TlNO_3$ and ANTS has a solubility product in the range that may be reached inside the vesicle: 100 mM $TlNO_3$ × 30 mM ANTS precipitates while 50 mM $TlNO_3$ × 15 mM ANTS is soluble. Therefore, 3 mM ANTS, rather than 30 mM ANTS, was used to permit efflux of Tl^+ from the vesicle interior after it initially accumulated. Also, the shape of the quench curve (Figure 2) was considered. By setting $[Na^+_i]$ at ≤40 mM, incremental changes in $[Tl^+_i]$, as it accumulated in the vesicle and subsequently was lost during dissipation, were more nearly proportional to the changes in the fluorescence. In other experiments where $[Na^+_i] > 100$ mM, the response was attenuated.

Effects of External Tl^+ on Stimulated and Background Quench Signals. Figure 5 compares quench signals obtained in the absence (left column) and presence (right column) of a diffusion potential, as the $[Tl^+_o]$ was increased. As expected, when external $[Tl^+]$ was raised in the absence of a diffusion potential, both the leak and the BTX-activated signal were increased, although the ratio of activated to control quenching was not improved. When diffusion potentials were imposed, the background control quenching was moderately affected. The control leak was somewhat enhanced at the lowest external Tl^+ concentration and actually slightly reduced at the highest Tl^+ levels. These small effects are consistent with the expectation that the background leaks are poorly ion selective. In the BTX-stimulated samples, however, imposing a diffusion potential greatly enhanced the signal at all Tl^+ concentrations tested. The net signal and ratio of signal to background were both improved. The largest net signal was obtained at the highest Tl^+ concentration, while the highest signal-to-background ratio was at the lowest Tl^+ level tested.

Toxin-Modified Fluorescence Quench. The optimized assay provides a measure of alkaloid toxin activation and guanidinium toxin block of Na channels comparable to that from $^{22}Na^+$ uptake assays (see Figure 1). In the experiment illustrated in Figure 6, both BTX (left panel, b, 5 μM) and VTN (righ panel, b, 100 μM) stimulated fluorescence quench above control levels (both panels, a). External TTX (1 μM) partially inhibited the signal (both panels, c), and external plus internal TTX (1 μM) blocked more completely (left panel, d). The magnitude of the stimulation can be simply assessed at any given time by comparing the amplitude of the stimulated quench to the control quench. These numbers, analogous to those from radiotracer studies, indicate that BTX stimulated quench by 5–8-fold, while VTN stimulated quench by ~3-fold. However, use of simple maxima does not in all cases provide a quantitative index of channel activation. More information may be obtained by analyzing the kinetics of the entire time course.

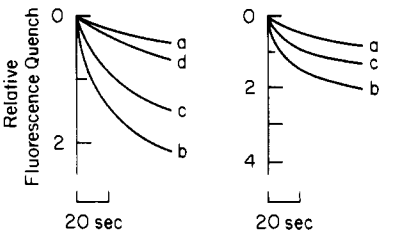

FIGURE 6: Neurotoxin-stimulated fluorescence quenching. (Left panel) Vesicles containing 3 mM ANTS were treated with (a) 1% ethanol vehicle, (b) 5 μM BTX, (c) 5 μM BTX + 1 μM TTX external, or (d) 5 μM BTX + 1 μM TTX internal and external, i.e., added before FTS. (Right panel) Vesicles containing 30 mM ANTS were treated with (a) Tris-SO_4 vehicle, (b) 100 μM veratridine, or (c) 100 μM veratridine + 1 μM TTX external. In both experiments, toxin-treated samples were stripped of external Na^+, and fluorescence was measured in 40 mM $TlNO_3$. Curves represent chart recorder tracings from superimposed triplicate time courses.

Kinetic Analysis of the Quench Reaction. In order to extract a parameter from the time course that is proportional to channel activity, we have derived equations which describe the time course of Tl^+ influx into a suspension of vesicles in the presence of a diffusion potential. The Stern–Volmer relationship then is used to transform the Tl^+ concentration into an effect on fluorescence. The resulting equation permits the time course to be linearized. The kinetics are completely described by three parameters, which specify an amplitude of quench at infinite time, $[(F_0 - F_\infty)/F_0)$, and a time constant for attaining that quench, τ; each of these parameters is obtained unambiguously from the linear replot. The origins of the equations used here are discussed in the Mathematical Appendix. The time course of Tl^+ influx is described by an exponential relationship of the form

$$[Tl^+_i]_t = [Tl^+_i]_\infty[1 - \exp(-t/\tau)] \quad (2)$$

where $[Tl^+_i]_t$ is the concentration of Tl_+ inside at time t, $[Tl^+_i]_\infty$ is the internal Tl^+ concentration as $t \rightarrow \infty$, and τ is the time constant for equilibration.

As discussed in the Mathematical Appendix, under the standard assay conditions, with no external permeant cations other than Tl^+, the maximal level of internal Tl^+ is set by the initial internal Na^+ concentration ($[Tl^+_i]_\infty = [Na^+_i]_0$), and this should be insensitive to the external Tl^+ concentration. On the other hand, the time constant should be inversely proportional to the external Tl^+ levels ($\tau^{-1} = k_1[Tl^+_o]$, where k_1 is an apparent second-order equilibration rate constant). This accounts for the enhancement in quench rate with increasing Tl^+ in the right-hand column of traces in Figure 5. When this equation is combined with the Stern–Volmer relationship (eq 1) by substituting $[Tl_i]_t = (F^0 - F_t)/(K_sF_t)$ and $[Tl_i]_\infty = (F^0$

$- F_\infty)/(K_s F_\infty)$, K_s drops out. Rearranging, we find that fluorescence at any time t, F_t, is given by

$$F_t = \frac{F_\infty}{1 - \left(\frac{F_0 - F_\infty}{F_0}\right) \exp(-t/\tau)} \quad (3)$$

where F_0 is the fluorescence at $t = 0$ and F_∞ is the fluorescence as $t \rightarrow \infty$. This equation may be rearranged to a form that linearizes that time course of the quench reaction:

$$\ln\left(\frac{F_t - F_\infty}{F_t}\right) = \ln\left(\frac{F_0 - F_\infty}{F_0}\right) - (t/\tau) \quad (4)$$

The use of eq 4 to analyze the time course is outlined in the Mathematical Appendix. Briefly, the data are scaled as described under Materials and Methods [and see Figure 10 in the Mathematical Appendix), F_∞ is estimated by inspection, and a plot is made of ln $[(F_t - F_\infty)/F_t]$ vs. t. Only when an accurate estimate of F_∞ is used will the replotted data be linear at later time points. By extending the analysis to longer times, the fit may be made arbitrarily precise. Once a satisfactory estimate of F_∞ is obtained by iteration, τ is the negative reciprocal of the slope. The y intercept of the extrapolated data is ln $[(F_0 - F_\infty)/F_0]$ and should be in agreement with the iterated value of F_∞ and $F_0 = 1$. There are no adjustable parameters in the graphical analysis of the data, and F_∞, F_0, and τ are unambiguously obtained. The terms $[(F_0 - F_\infty)/F_0]$ and τ may be used in eq 3 to regenerate a calculated fluorescence time course for comparison with the original data.

The term $[(F_0 - F_\infty)/F_0]$ reflects the fraction of vesicles participating in the quench reaction as well as the magnitude of the maximum quench level in each vesicle. τ is a measure of the rate at which the average participating vesicle is equilibrated. This latter term therefore is a measure of the channel activity per vesicle. When channels are sparse (i.e., ≤ 1 channel per vesicle), the fraction of vesicles activated is proportional to the fractional channel activation. When channels are abundant, however, the fractional activation should be inversely proportional to the time constant but not directly related to the fraction of vesicles participating.

Application of the Kinetic Model. Figure 7 illustrates the use of the equations to analyze the quench time courses from Figure 6. Panels A and B are the linear replots from eq 4 of the BTX and VTN data, respectively. The symbol × here corresponds to trace a in Figure 6, Δ to trace b, and O to trace c. The values for F_∞ and τ derived from these plots, as listed in the figure legend, were used in eq 3 to calculate the theoretical time courses. These have been superimposed (solid symbols) in panels C and D over the actual traces (dashed lines). All the curves were well fit, especially at later times as F_∞ was approached. A deviation occurred at early times in the theoretical time courses for BTX (panel C) and VTN (not shown). This could be predicted from the linear replots; in each case the line does not extrapolate exactly to the plotted value at $t = 0$. Because this y intercept equals $[(F_0 - F_\infty)/F_0]$ and the theoretical time courses demonstrated that the estimate of F_∞ is valid, the value of F_0 must not equal 1. When the extrapolated value of F_0 (0.952) from the VTN linear replot was used in calculating the theoretical time course (open circles, panel D), an excellent fit resulted. Such an offset in F_0, which is sometimes observed at high concentrations of activating toxin, appears to be caused by an initial rapid phase of quench that was complete in the first few seconds of recording (cf. Figure 10C in the Mathematical Appendix). This is most likely due to a subpopulation of vesicles of either small

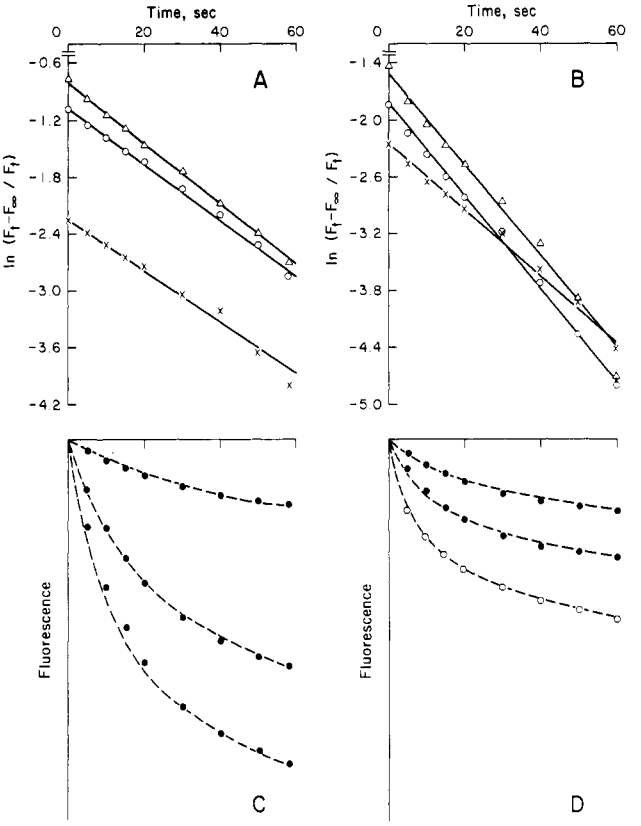

FIGURE 7: Kinetic analysis of quench signals. (A and B) Data from Figure 6 were linearized by using eq 4 with $F_0 = 1$. In (A) Δ = 5 μM BTX, $F_\infty = 0.535$, $\tau = 31.3$ s, and $F_t = 0.574$ at $t = 58$ s; O = 5 μM BTX + 1 μM TTX external, $F_\infty = 0.660$, and $\tau = 33.7$ s; × = 1% ethanol vehicle, $F_\infty = 0.895$, and $\tau = 37.2$ s. In (B) Δ = 100 μM VTN, $F_\infty = 0.760$, $\tau = 21.0$ s, and $F_t = 0.767$ at $t = 60$ s; O = 100 μM VTN + 1 μM TTX, $F_\infty = 0.840$, and $\tau = 20.6$ s; × = isosmolar Tris-SO_4 vehicle, $F_\infty = 0.895$, and $\tau = 28.8$ s. (C and D) Data from Figure 6 are replotted as dashed lines, superimposed by theoretical F_t values (●) determined by inserting the values for F_∞ and τ, listed above, into eq 3. For the VTN curve, theoretical F_t values (O) were determined by using $F_0 = 0.952$.

volume or high channel density that equilibrates rapidly and therefore does not contribute to the kinetics throughout the time course. As seen most clearly by inspection of panel A of Figure 7, τ is not a good indicator of channel activity, as the slope of the replots was nearly equal for different toxin conditions. The value of F_∞, however, changed markedly as a function of the channel activity state. This may be interpreted as changes in the number of vesicles participating in the quench reaction. Employing the value of $(F_0 - F_\infty)$ as a measure of channel activity, BTX stimulated by 4.4-fold above the control and VTN stimulated by 2.3-fold above its control.

Ionic Dependence of Quench Kinetics. As discussed above, the generation of a diffusion potential should cause $[Tl^+_i]_\infty$ to be "set" by $[Na^+_i]_0$. Without such a potential, internal and external solutions would equilibrate and $[Tl^+_i]_\infty$ would merely rise to $[Tl^+_o]$. This was tested with vesicles loaded with 185 mM Na^+. Samples treated with BTX or ethanol vehicle were assayed against 10, 15, 20, or 25 mM Tl^+. The diffusion potential was held approximately constant by balancing reductions in external Tl^+ with addition of Na^+. Cation concentrations were selected to take advantage of different portions of the Stern–Volmer curve (Figure 2). If Tl^+ were merely equilibrating, the range from 10 to 25 mM Tl^+ would result in quite different values of F_∞. However, if there were electroneutral concentration, the final level of $[Tl^+_i]_\infty$ would approximate the product of $[[Tl^+_o]/([Na^+_o] + [Tl^+_o])] \times 185$

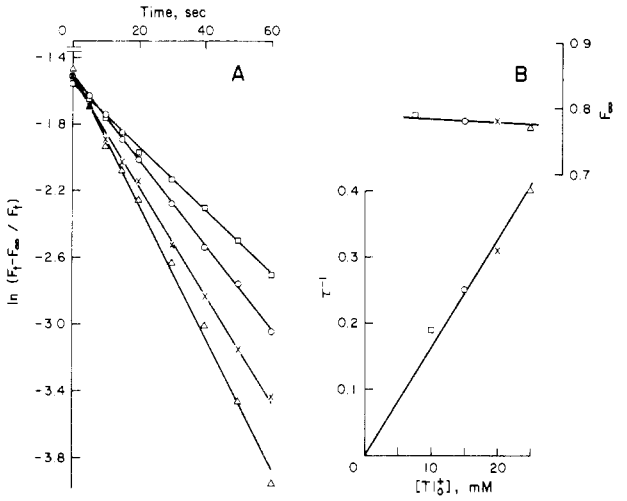

FIGURE 8: Final amplitude of quench signal is independent of external $[Tl^+]$. Vesicles as in Figure 1, but including 3 mM ANTS (so $[Na^+_i] \sim 185$ mM), were incubated ± 2.5 μM BTX, stripped of external Na^+, and assayed in various concentrations of $TlNO_3 + NaNO_3$ (isosmolar in Tris-SO_4). Difference curves (BTX minus control) were calculated from averages of triplicate time courses. In panel A, results with (□) 10 mM $TlNO_3$ + 15 mM $NaNO_3$, (○) 15 mM $TlNO_3$ + 10 mM $NaNO_3$, (×) 20 mM $TlNO_3$ + 5 mM $NaNO_3$, and (△) 25 mM $TlNO_3$ were linearized according to eq 4. In panel B, the values thus determined for F_∞ and slope (τ^{-1}, in $s^{-1} \times 10$) were plotted as a function of $[Tl^+_o]$. Note that F_∞ varied insignificantly as $[Tl^+_o]$ changed, whereas the slope varied proportionally.

mM, ranging between 74 and 185 mM. Thus, the quench would be large and vary by only 10% in participating vesicles. The difference curves from the experimental time courses were analyzed according to eq 4 (Figure 8A), and the derived parameters were plotted against $[Tl^+_o]$ (Figure 8B). As predicted for electroneutral concentration, there was only a slight shift in F_∞ as a function of external thallous ion concentration.

The observed dependence of τ, the time constant for equilibration, on external Tl^+ concentration merits special comment. In general, under several ionic conditions, τ has always been found to decrease as external $[Tl^+]$ was raised. In the case of the standard assay, where Tl^+ is essentially the only permeant external ion (as in Figure 5), this dependency is expected [as seen by inspection of eq A8 in the Mathematical Appendix]; the relation between τ^{-1} and $[Tl^+_o]$ would not be expected to be perfectly linear (e.g., $\tau^{-1} \cong k_0[Tl^+_o]$) because of a voltage term in the equilibration rate "constant", k_0, which is affected weakly by the external Tl^+ concentration. However, in the present experiment, in which the total external concentration of permeant ions ($[Na^+_o] + [Tl^+_o]$) was constant, τ should be invariant with external $[Tl^+]$ [see eq A8, Mathematical Appendix], unless the permeability of the two ions is not exactly the same. As seen in Figure 8B, τ^{-1} varied directly with $[Tl^+_o]$. Variations in this direction may result if the permeability of Tl^+ were somewhat higher than that of Na^+. The nature of the true permeability ratio is a complex one, as exemplified by reports in the literature. While in studies of myelinated axons Hille (1972) estimated on the basis of reversal potentials that P_{Tl}/P_{Na} was 0.33, in reports with BTX-treated Na channels, Khodorov (1978) reported that the ratio was approximately 1.3, and studies conducted with neuroblastoma cells also indicated that BTX modified the permeability ratio, enhancing Tl^+ permeability relative to Na^+ (Huang et al., 1979). In addition, the permeability ratio may vary somewhat at different ionic concentrations if there are deviations from the independence principle (Hodgkin & Katz, 1949). We currently are investigating the selectivity of the reconstituted channel for Tl^+ under different ionic conditions and when activated by VTN as well as BTX. In any event, the empirical observation that the time constant varies as the reciprocal of the external Tl^+ concentration is an important consideration for optimizing the quench signal.

The dependence of F_∞ on varying $[Na^+_i]_0$ was also observed, although not studied systematically. These experimentas require preparation of different FTS samples with the same internal volume, which is difficult to achieve precisely. In experiments where vesicles were loaded with $[Na^+_i]$ ranging from 10 to 200 mM and tested against proportional $[Tl^+_o]$, F_∞ increased nonlinearly as the $[Na^+_i]$ decreased, as expected from the Stern–Volmer relationship (data not shown).

Quench Kinetics, Vesicle Dimensions, and Na Channel Abundance. The time courses of both radiotracer influx and fluorescence quenching take place in seconds to minutes. It is well recognized that the conductance of a single activated Na channel is sufficient to fully equilibrate a vesicle of 500–1000-Å diameter with 0.1 M Na^+, in tens of milliseconds (Miller, 1984). A concern, therefore, is that the slower kinetics could reflect the condition of the channels themselves. Solubilization, purification, and reconstitution could yield damaged channels that conduct poorly or rarely enter the activated state. Several kinds of evidence indicate that the channels actually conduct ions efficiently but that the suspension consists of very large vesicles with channels in fairly low abundance.

We have found that the time required to achieve any specified level of quench is inversely proportional to the external Tl^+ concentration (unpublished data). This indicates that the rates at which ions are entering the vesicles are being measured rather than the probability that channels are activated followed by sudden, complete equilibration of their associated vesicle.

Three lines of evidence show that PE/PS/PC vesicles are large after the standard FTS treatment. Examination of reconstituted vesicles by light microscopy revealed that the majority of those observed had diameters of 2–5 μm. As sonication was extended beyond 2 s (260-μL samples), diameters decreased to below 1 μm, eventually becoming submicroscopic. In addition, PE/PS/PC vesicles labeled with [^{14}C]PC were sized by gel filtration, following FTS (W. Bollinger, unpublished data). Under these conditions, 15–20% of the lipid was in particles of diameter >0.8 μm. Nearly all of the remaining vesicles had diameters >0.6 μm. Further, 90% of the BTX-activated quench was lost when reconstituted samples were first filtered through membranes having 0.8-μm exclusion limits. These observations indicate that virtually all of the vesicles contributing to the quench kinetics were 8000 Å in diameter or larger; vesicles of smaller dimensions with activated channels and very rapid quench kinetics may account for the occasional offset between the extrapolated and measured values of F_0 mentioned above.

Two kinds of evidence are consistent with low channel densities (channels per vesicle <1) in the reconstituted vesicles. First, half of the BTX-activated quench was blocked by saturating concentrations of external TTX, which should only act at channels oriented outside out (see Table II, and Figure 6). Vesicles containing many randomly oriented channels would be fully equilibrated by even a single unblocked channel. Second, this argument is based on the effects of toxins on F_∞ and τ. At high channel surface densities, the time constant for equilibration, τ, should be sensitive to the concentration of activating toxin (e.g., BTX). The numbers of channels activated per vesicle, and therefore τ^{-1}, would increase as a function of toxin occupancy. Under these conditions, F_∞, reflecting the total number of vesicles activated, would be

Table I: $K_{1/2}$ Values for Na Channel Specific Toxins

preparation (ref)	VTN (μM)	BTX (nM)	TTX (nM)
reconstituted eel electroplax (this paper)[a]	5.4 ± 2.0 SEM (3)[c]	169 ± 44 SD (2)	4.3[b] ± 2.1 SEM (3)
reconstituted eel electroplax (Rosenberg et al., 1984a)	18		33
reconstituted rat brain (Tamkun et al., 1984)	27.8	2000	14
reconstituted rat sarcolemma (Weigele & Barchi, 1982)	35	1500	
rat brain synaptosomes (Kreuger & Blaustein, 1980)	20	2000	
rat brain synaptosomes (Tamkun & Catterall, 1981)	13	500	
neuroblastoma (Catterall, 1977)	29	700	
frog node of Ranvier (Ulbricht, 1979)			3.6
soluble eel electroplax (Levinson et al., 1979)			7.2

[a] $K_{1/2}$ values determined from Eadie–Hofstee fits of fluorescence data. [b] Block of BTX-stimulated quench. [c] Standard error of the mean and number of experiments; each experimental n was the mean of $K_{1/2}$ values determined at 10, 20, 40, and 60 s and/or at F_∞.

essentially constant. If, however, each participating vesicle contained only one or a few channels, the time constant would be insensitive to toxin occupancy. Either each participating vesicle's channel would be unoccupied, and therefore not activated and the vesicle would not contribute to the signal, or it would be activated and the rate constant would reflect the equilibration by that single channel. In this case, however, the number of vesicles participating (and therefore F_∞) would vary with toxin occupancy. As noted previously (see Figure 7), activation or inhibition by toxins was best reflected by F_∞ and not τ, as expected if vesicles had low channel densities. While at high channel densities equilibration rates should scale as r^{-1}, at low abundance the rates should vary as r^{-3}. Thus, in the present case, a 1-μm diameter vesicle should follow kinetics 1000-fold slower than a vesicle of 1000-Å diameter.

Neurotoxin and Anesthetic Interactions Evaluated by Fluorescence Quench. The fluorescence assay, when optimized as described, may be used to analyze the biochemical pharmacology of the reconstituted channel. Figure 9 shows dose–response curves for VTN (A), BTX (B), and TTX (C); the data have been treated in different ways for illustration. The effects of various VTN concentrations on quench were assessed as the differences in amplitude between VTN-treated vesicles and controls measured at 60 s. This approximates ($F_0 - F_\infty$) but is partly lacking in precision because the measurement does not extract information from all time points. Each sample was assayed in triplicate, and the bars denote standard propagated error of the mean differences. The data were well fit by a Langmuir isotherm with $K_{1/2}$ of 5.4 μM. In Figure 9B, BTX-stimulated quench at different concentrations was assessed at 10, 20, 40, and 60 s, and the data were normalized by setting the signal at 5 μM BTX equal to 100%. The close correspondence of these normalized dose–response data from different points in the time course indicates that τ was invariant as expected for vesicles with low channel densities, again underlining that F_∞ is the best index of channel activation. The best fit Langmuir isotherm yielded a $K_{1/2}$ of 200 nM. In Figure 9C, TTX inhibition of BTX-stimulated quench was determined from the F_∞ values of the averaged differences at each TTX concentration determined with eq 4. In this experiment, stimulated quench was inhibited a maximum of 60% by external TTX, with a $K_{1/2}$ of 0.7 nM.

It should be mentioned that Tl^+ has been reported to bind competitively at the TTX and STX binding site ($K_i \sim 20$ mM; Henderson et al., 1974). This may interfere with measurements of the STX block of the channel, because STX equilibrates rapidly in comparison with the 1-min time course of flux measurements. However, for the electroplax channel, not only in solubilized preparations (Agnew et al., 1978; Levinson et al., 1979) but also in native and reconstituted membranes (unpublished data), TTX dissociates with a half-life of 25–30 min. It was thus expected that Tl^+ would not interfere with TTX preequilibrated with the vesicles before assay. Consistent with this, in a set of matched dose–response curves, the $K_{1/2}$ values for TTX inhibition of BTX-stimulated fluorescence quench were the same ($n = 1$) in either 8 or 40 mM Tl^+.

Table II: Inhibition of BTX-Stimulated Fluorescence Quench by TTX and Local Anesthetics[a]

drug (concn)	% inhibition
TTX_{i+o} (1 μM)	91.7 ± 3.5 (6)
$QX\text{-}222_{i+o}$ (3 mM)	75.4 ± 5.0 (4)
$dibucaine_o$ (0.1 mM)	80.8 ± 3.3 (11)
$tetracaine_o$ (0.1 mM)	73.6 ± 4.4 (4)
TTX_o (1 μM)	51.0 ± 5.5 (7)
$QX\text{-}222_o$ (3 mM)	45.1 ± 4.4 (7)
TTX_o (1 μM) + $QX\text{-}222_o$ (3 mM)	72.0 ± 3.7 (7)

[a] For equilibration inside and outside (i + o), toxins were added to the vesicles before FTS and supplemented to the external solution at the appropriate concentration after dilution steps. Drugs tested externally (o) were preincubated with the vesicles for 12 min at 0 °C. In both cases, vesicles were incubated 36 min at 30 °C ± 5 μM BTX. Each sample was assayed in triplicate and the average difference curve calculated. Data are expressed as percent inhibition ± SEM (n); each experimental n was the mean of the fluorescence determined at 10, 20, 40, and 60 s and/or at F_∞. Values for external TTX and QX-222 were determined in the same experiments.

The average $K_{1/2}$ for each toxin determined from several fluorescence experiments is presented in Table I. Listed for comparison are values from the literature, including results from studies of Na channels from other tissues. The $K_{1/2}$ values for VTN, 5.4 μM, and TTX, 4.3 nM, are both lower than we previously reported (Rosenberg et al., 1984a). This at least in part reflects variations among different starting native membrane preparations. Affinities for both toxins are in the expected range. The $K_{1/2}$ for BTX of 169 nM is the lowest reported for reconstituted Na channels and compares favorably with the lower values for channels in native membrane environments.

The ability of assorted inhibitors to block BTX-stimulated quench is summarized in Table II. Effects of TTX and local anesthetics were measured to assess the degree to which the sites have been preserved and the orientation of the sites across the membrane. When a saturating concentration of TTX was equilibrated with both sides of the membrane, most or all of the stimulated quench was blocked, suggesting that few channels retaining the functional BTX binding site failed to be inhibited with TTX. It was sometimes observed that TTX blocked a percentage of the control quench (also observed in some radiotracer studies; unpublished data), suggesting that some channels may be open in the absence of activating neurotoxins, yet still retain functional TTX binding sites.

Retention of the local anesthetic binding site was demonstrated by the inhibition of flux with dibucaine and tetracaine (both membrane permeant) and by QX-222 (membrane impermeant) equilibrated with both sides of the membrane. Again, a portion of the basal quench was sometimes inhibited by the local anesthetics, and this was seen also in radiotracer

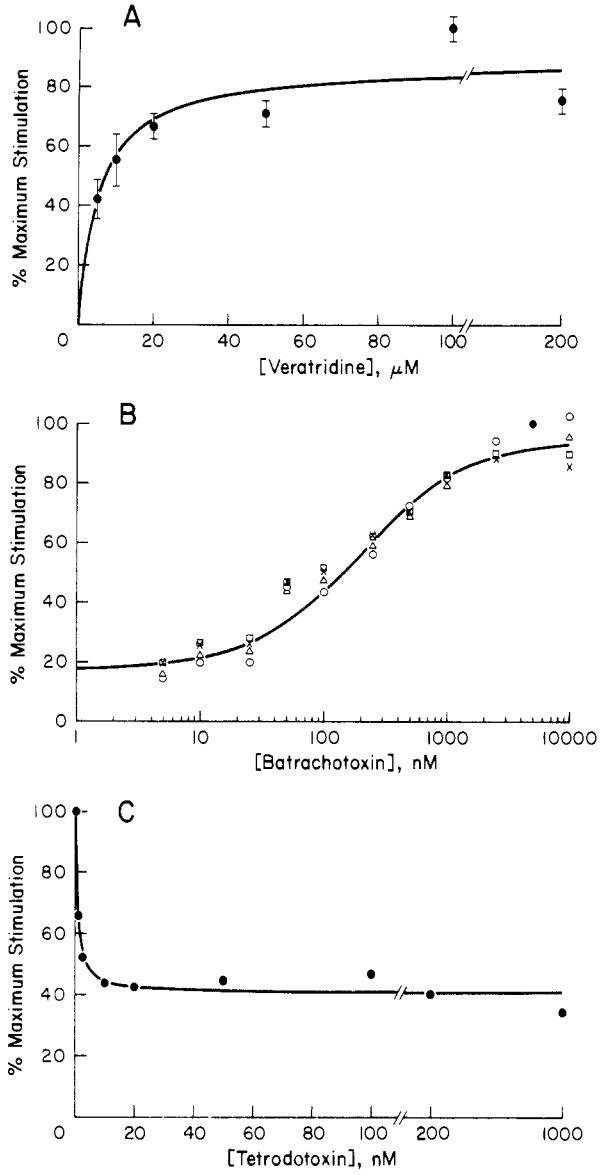

FIGURE 9: Dose–response curves determined by fluorescence quench. Vesicles loaded with ~185 mM Na^+ + 3 mM ANTS were stripped of external Na^+ after incubation with toxins and assayed in 40 mM $TlNO_3$. (A) Vesicles were incubated for 6 min at 30 °C ± VTN. Difference curves were determined from triplicate averages after 60 s of Tl^+ influx. Stimulated quench in 100 μM VTN was set to 100%. Bars denote standard propagated error of the means. An Eadie–Hofstee fit of the data yielded K_d = 5.4 μM and maximum stimulation of 87.8%. These parameters were used to generate the Langmuir isotherm shown. (B) Vesicles were incubated for 36 min at 30 °C ± BTX. Difference curves were determined from triplicate averages at (○) 10, (△) 20, (□) 40, and (×) 60 s of Tl^+ influx. Stimulated quench in 5 μM BTX at all times was set to 100% (●). Data were best fit by a Langmuir isotherm with maximum stimulation set to 95%, base line effect in the absence of BTX set to 18%, and K_d = 200 nM to yield the curve shown. (C) Vesicles were incubated for 12 min at 0 °C with TTX and then 36 min at 30 °C ± 5 μM BTX. Difference curves from triplicate averages were linearized by eq 4 to determine F_∞. An Eadie–Hofstee fit of the F_∞ data yielded K_d = 0.7 nM and maximum inhibition of 59.3%. These parameters were used to generate the Langmuir isotherm shown.

experiments (unpublished data), indicating that some preparations may contain chronically open channels. In addition, apparent incomplete block of the BTX-stimulated signal by the lipophilic anesthetics is not fully understood. In our experiments, small amounts of membrane lipid are incubated with the drug. At anesthetic concentrations that may be appropriate for physiological studies, it might be expected that the intramembrane concentration would be high enough not only to block the channel but also to produce a nonspecific leak in the vesicles. However, this would also appear in controls treated with the anesthetic alone, in the absence of BTX; such an effect is not consistently found.

Table III: Estimates of Single-Channel Conductance[a]

toxin (μM)	$[Na^+_i]$ (mM)	$[Tl^+_o]$ (mM)	τ (s)	γ (pS)
BTX (5)	40	40	15.7	2.6[b] – 40.7[c]
VTN (100)	40	40	16.5	2.5 – 38.7
VTN (100)	10	10	17.0	0.6 – 9.4

[a] Vesicles loaded with $[Na^+_i]$ indicated, including 2.5 or 3 mM ANTS, were incubated ± toxin, stripped of external Na^+, and assayed in triplicate in $[Tl^+_o]$ indicated. Difference curves for each toxin were calculated and F_∞ and τ determined. [b,c] Average vesicle diameters of 0.8 or 2.0 μm were used to calculate single-channel conductance, γ, from eq A11, $\gamma_{(c_j)} = [v_i z^2 F^2 c_{(j)}]/(n\tau RT)$, where v_i is intravesicular volume, $c_{(j)}$ is concentration of the jth ion, and other terms have their standard meaning.

When QX-222 was incubated with the external surface only, partial quench inhibition was observed. When equilibrated with both sides, inhibition was greater (75.4% vs. 45.1%). This is consistent with the expectation that the QX-222 site is accessible from just one side of the membrane. When 3 mM external QX-222 and 1 μM external TTX were both added, the block was 72%, as expected if the two binding sites were exposed on opposite sides of the membrane, permitting the compounds to act on oppositely oriented channels. The interactions of several types of local anesthetics with membranes and sites on the channel are currently under further investigation.

Estimate of the Single-Channel Conductance. When measured in the absence of a diffusion potential, the time constant of quenching, τ, can be used to estimate single-channel conductance, γ, if certain assumptions can be made (see Mathematical Appendix). It was concluded above that few vesicles have more than one channel. Activated channels are presumed to be chronically opened, and the permeability and activity of Tl^+ are assumed to be approximately equal to those of Na^+. Measurements were made of τ under conditions where $[Na^+_i]$ and $[Tl^+_o]$ were equal. Estimates of the single-channel conductance were made from three experiments with BTX or VTN as activating toxins, assuming the average vesicle diameter was either 0.8 or 2 μm, as shown in Table III. Values estimated are between 0.6 and 40.7 pS, representing fluxes of (1.2×10^5) to (8.1×10^6) ions s^{-1} $channel^{-1}$, under the ionic conditions of assay. Given the imprecision of the assumptions, this range is in good agreement with the 10–25 pS recorded for BTX-treated Na channels in native membranes and planar bilayers (Krueger et al., 1983; Huang et al., 1984; Hartshorne et al., 1985).

CONCLUSIONS

We have described a fluorescence quench assay for the study of the voltage-regulated Na channel in reconstituted vesicle preparations. The assay employs a water-soluble, highly fluorescent reporter group trapped in the interior of reconstituted liposomes. The heavy-metal ion Tl^+ substitutes for Na^+ in passing through activated Na channels and quenches the internalized fluorophore in a concentration-dependent manner. The signal is exaggerated through the use of diffusion potentials, which result in the concentration of Tl^+ preferentially in vesicles containing the activated, cation-selective channel. Such imposed voltage gradients may be exploited in the future to examine the gating behavior of the toxin-activated channel. The time course is extended to the scale of

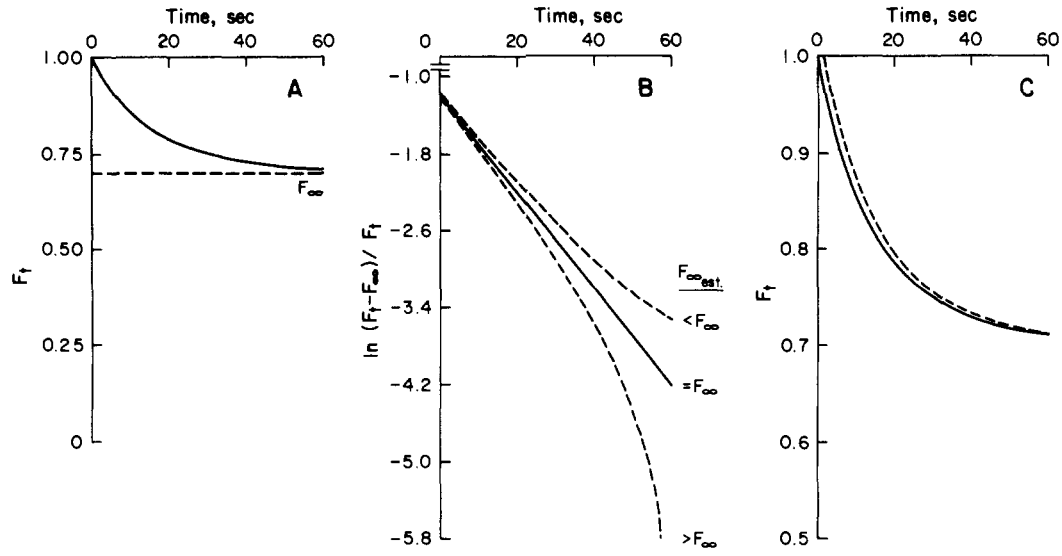

FIGURE 10: Graphical and theoretical considerations in kinetic analysis of fluorescence time courses. (A) Arbitrary scaling of representative time course. Fluorescence at $t = 0$, F_0, is set = 1.00. A reference point is designated and set at 0. An estimate of fluorescence at infinite time, F_∞, is made on the basis of the amplitude of the curve at 60 s and its rate of change. Plotted curve calculated from eq 3 with $F_\infty = 0.700$ and $\tau = 20$ s. (B) Linearization plot of ln $[(F_t - F_\infty)/F_t]$ vs. time from eq 4. If the estimated F_∞ from (A) deviates from the true F_∞, the linear replot will deviate as shown. Data from (A) were analyzed with estimated $F_\infty = 0.69$, 0.70, or 0.71. (C) Time course from (A) drawn in solid lines at expanded scale. For comparison, a time course calculated from eq 3 with the same F_∞ (0.70) but an offset in F_0 (1.05) is drawn in dashed lines. The curves deviate progressively less as the time course proceeds.

seconds through the use of large liposomes (diameter ~0.8–5 μm), formed by appropriate mixtures of lipid in a freeze–thaw–sonication cycle. This circumvents the need for a specialized stopped-flow apparatus to resolve transport rates.

This assay represents a significant advance over radiotracer assays. Each continuous time course consumes approximately 1–10 fmol of active protein, about 100 times less than required for a four-point time course measured with the $^{22}Na^+$ assay we have used previously. Thus, a reconstituted preparation of 500–750 pmol of Na channel is seldom fully consumed during the more than 3 weeks it is active. Furthermore, the assays are rapid, requiring one person 6 min to complete each set of triplicate time course measurements. Data acquisition and analysis can be readily computerized, making each experiment rapid to evaluate. The small scale of the incubations should assist in convserving limited supplies of valuable toxins, such as BTX.

The kinetic analysis is based on a straightforward physical model and yields two relevant terms, a maximum signal, $(F_0 - F_\infty)$, and a time constant, τ. Under the standard conditions, the maximum level of quenching in each vesicle is set by the initial internal Na^+ concentration, is independent of external Tl^+ concentration, and, together with the number of participating vesicles, determines the maximum signal. The time constant is inversely proportional to external Tl^+ and the number of activated channels per participating vesicle. Under the reconstitution conditions used here, with few channels per vesicle, the maximum signal reflects fractional channel activation. In future studies aimed at optimizing reconstitution, a dependence of the time constant and an independence of the amplitude on toxin concentrations will provide an index of increased surface densities of channels. Thus far, the assay has provided detailed dose–response information for BTX, VTN, and TTX. It will permit rapid screening of other drugs and toxins for interactions with the channel and will be useful in chemical modification studies directed at discovery of domains on the channel responsible for drug binding, gating activity, or transport mechanisms.

ACKNOWLEDGMENTS

We especially thank Dr. John Daly for gifts of BTX that made these experiments possible. We also thank Dr. W. Boron for use of a vapor pressure osmometer, Dr. J. Bertino for use of a spectrofluorometer, Dr. G. Rudnick for use of a fluorometer, and E. Brosius, Yale glassblower, for construction of Y connectors.

MATHEMATICAL APPENDIX

The time course for quench development is quantitatively described by eq 3 and 4. The origin of these equations is developed here.

Kinetics of Tl^+ Influx. To describe Tl^+ influx in the presence of a diffusion potential, we consider the behavior of an ideal unilamellar liposome that, aside from the conductance induced by channel activation, is not leaky to ions. We have assumed that Tl^+ enters the vesicle by electroneutral exchange for internal Na^+ with essentially no net cation transport; this is justified by the following calculation. After removal of external Na^+ and other permeant cations, net Na^+ efflux should occur until a diffusion potential equal to the Na^+ reversal potential is established. On mixing with low external Tl^+, only exchange should then take place. (Over longer times, of course, the entire collection of ionic gradients will dissipate.) If the average vesicle has a 1-μm diameter, the surface area and internal volume would be 3.1×10^{-8} cm^2 and 5.2×10^{-13} cm^3, respectively. For a 100-fold Na^+ concentration gradient, at 20 °C, the reversal potential would be 0.116 V. If membrane capacitance is ~1 μF/cm^2, a potential of this magnitude would develop after net efflux of 3.6×10^{-15} C, or about 2.3×10^5 ions. If the internal Na^+ concentration were initially 0.15 M, this efflux would represent less than 0.5% of the internal pool.

Because Na/Na and Tl/Tl exchanges are without consequence for the quench signal, only Na/Tl exchange need be described, and that reaction should be

$$Tl_o + Na_i \underset{k_2}{\overset{k_1}{\rightleftharpoons}} Tl_i + Na_o$$

From the electroneutral exchange assumption (e.g., $d[Na_i]/dt$

$= -d[Tl_i]/dt$), it follows that $[Na_i]_0 = [Tl_i]_t + [Na_i]_t$, where the subscripts within the brackets correspond to i = inside and o = outside and those outside correspond to time $t = 0$ or any time t. The integrated rate equation for the time course is

$$[Tl_i]_t = \frac{k_1[Tl_o]}{k_1[Tl_o] + k_2[Na_o]}[Na_i]_0 \times \left[1 - \exp\left[-\left(\frac{k_1}{v}[Tl_o] + \frac{k_2}{v}[Na_o]\right)t\right]\right] \quad (A1)$$

where k_1/v and k_2/v are the apparent second-order rate constants divided by the vesicular volume, v. Under the standard assay conditions where there is no external Na^+, A1 simplifies to

$$[Tl_i]_t = [Na_i]_0\left[1 - \exp\left(-\frac{k_1}{v}[Tl_o]t\right)\right] \quad (A2)$$

As $t \rightarrow \infty$, it becomes evident that $[Ti_i]_\infty = [Na_i]_0$ and substituting $\tau^{-1} = (k_1/v)[Tl_o]$ yields eq 2.

These relationships show that the time constant, τ, is inversely proportional to $[Tl_o]$. Further, the maximum internal Tl^+ would be "set" by the initial $[Na_i]$ and would not be affected by $[Tl_o]$. If there were no electroneutral exchange, the internal solution would merely equilibrate with the external and $[Tl_i]_\infty = [Tl_o]$.

Relationship to Classical Equations of Electrochemistry. Equation A2 is intuitively appealing but is not rigorously derived. The rate "constants", for example, may be affected by voltage and therefore not be independent of permeability coefficients or concentration gradients; thus, $[Na_i]_0$ would be found in k_1. An alternative derivation, yielding equations of the same general form, may be drawn from the classical treatment of ionic fluxes by Goldman (1943) and Hodgkin and Katz (1949).

Adopting the original sign convention of Hodgkin and Katz (1949), inward current of the jth cation species (I_j) and the potential (E_m) which drives an inward cation current are both positive. Thus

$$E_m = \frac{RT}{zF}\ln\left(\frac{\sum P_j a_{(j)i}}{\sum P_j a_{(j)o}}\right) \quad (A3)$$

where E_m is the transmembrane voltage when total current $I = 0$ and P_j and $a_{(j)}$ are the permeability coefficient and activity for ion j, respectively; the subscripts refer to inside (i) or outside (o) the compartment. Equations 2.3–2.5 of Hodgkin and Katz (1949) show the current density of the jth species to be

$$I_j = \frac{z^2F^2}{RT}P_jE_m\left[\frac{a_{(j)o} - a_{(j)i}\exp\left(-\frac{zFE_m}{RT}\right)}{1 - \exp\left(-\frac{zFE_m}{RT}\right)}\right] \quad (A4)$$

where z, F, R, and T have their usual meanings. Because we are describing a vesicle in which conductance is almost entirely through activated channels, P_j is approximately the product of the number of channels times the individual contributions of each channel to the permeability. Thus, I_j becomes the current per vesicle rather than current per unit membrane area. Setting $da_{(j)i}/dt = I_j/zFv$, then if the activity of the external ion ($a_{(j)o}$) is constant, and the initial internal concentration $a_{(j)i} = 0$, the integrated rate equation is

$$a_{(j)i} = \frac{k_i}{k_o}a_{(j)o}[1 - \exp(-k_o t)] \quad (A5)$$

where

$$k_i = \frac{zF}{vRT}P_j\left[\frac{E_m}{\exp\left(\frac{zFE_m}{RT}\right) - 1}\right]$$

and

$$k_o = \frac{zF}{vRT}P_j\left[\frac{E_m}{1 - \exp\left(\frac{-zFE_m}{RT}\right)}\right]$$

By reintroducing the definition of E_m, together with the electroneutrality constraint that $[Na_i]_0 = [Tl_i]_t + [Na_i]_t$, and equating activity to concentration, we find

$$k_o = \frac{\left(\frac{zFE_m}{RT}\right)P_{Tl}(P_{Tl}[Tl_o] + P_{Na}[Na_o])}{(P_{Tl} - P_{Na})[Tl_i] + P_{Na}[Na_i]_0 - P_{Tl}[Tl_o] - P_{Na}[Na_o]} \quad (A6)$$

Equation A5 then becomes

$$[Tl_i]_t = \frac{[Tl_o][Na_i]_0\left[1 - \exp\left(-\frac{k_o}{v}t\right)\right]}{[Na_o] + [Tl_o] + \left[\left[\left(\frac{P_{Tl}}{P_{Na}}\right) - 1\right]\exp\left(-\frac{k_o}{v}t\right)\right]} \quad (A7)$$

If, for the moment, we assume that $P_{Tl} \cong P_{Na}$, this becomes

$$[Tl_i]_t = \frac{[Tl_o]}{[Tl_o] + [Na_o]}[Na_i]_0 \times \left[1 - \exp\left(\frac{-zFE_m}{vRT}\right)P_{Tl}\left(\frac{[Tl_o] + [Na_o]}{[Na_i]_0 - [Tl_o] - [Na_o]}\right)t\right] \quad (A8)$$

This equation provides much of the additional information missing from eq A1. As with eq A2, when $[Na_o] = 0$, $[Tl_i]_\infty = [Na_i]_0$. Also, under these conditions the time constant will be inversely proportional to $[Tl_o]$, though imperfectly because $[Tl_o]$ appears as a term in the denominator and E_m. The time constant will decrease as the vesicle permeability (number of activated channels) increases and as vesicle volume decreases. Further, differentiating this equation leads to the result assumed ab initio in eq A1, namely, that transport of Tl^+ into or out of the vesicles is proportional to the Tl^+ concentration on the "source" side and to the Na^+ concentration on the "destination" side of the membrane.

Equations A6 and A7 also predict that if P_{Tl} and P_{Na} are not approximately equal, both the apparent time constant and the preexponential term would vary during the course of the reaction. The limits of these, estimated for early and late times, reveal that the preexponential term will be most sensitive to differences in the two permeability coefficients. In our experiments the kinetic parameters appear to be constant throughout the time course (with the exception that small, very rapid phases of quenching are sometimes detected within the first few seconds, as mentioned below). Thus, invoking an equation of the form of eq A8 and A2, and thus eq 2, seems well justified.

Estimation of Single-Channel Conductances. From eq A4, in symmetrical ionic concentrations [e.g., $a_{(j)i} = a_{(j)o}$], it is evident that

$$I_j = \frac{z^2F^2}{RT}P_j a_{(j)} E_m = n\gamma_{(a_j)} E_m \qquad (A9)$$

The second equality is simply a form of Ohm's law, stating that conductance of the membrane is given by the number of activated channels (n) times the single-channel conductance at the ionic activity used [$\gamma_{(a_j)}$]. From eq A5, the equilibration time constant of a radioisotope of the permeant ion is merely $\tau = k_o^{-1}$, which thus becomes

$$\tau = \frac{zFv_i a_{(j)}}{n\gamma_{(a_j)}}\left[\frac{1 - \exp\left(-\frac{zFE_m}{RT}\right)}{E_m}\right] \qquad (A10)$$

When voltage $\rightarrow 0$, $E_m/[1 - \exp(-zEF/RT)] \rightarrow RT/zF$. Thus

$$\tau = \frac{v_i z^2 F^2 a_{(j)}}{n\gamma_{(a_j)} RT} \qquad (A11)$$

Thus, if we make the rough approximation that Tl^+ behaves as a tracer for Na^+ (i.e., $P_{Tl} \sim P_{Na}$), making reasonable assumptions about the vesicle radius permits an estimation of single-channel conductance. Given quantitative uncertainties in the assumptions, these estimates cannot be reliable to less than 1 order of magnitude.

Use of Equations 3 and 4. F_0 is measured from an arbitrary reference that can be absolute zero but is always less than F_∞; F_0 is scaled to have a value of 1.0 (Figure 10A). F_∞ is obtained by iteration. F_∞ is first estimated by inspection, and this value is used in eq 4 to transform the data. The transformed data are plotted against time (Figure 10B). If F_∞ is accurately chosen, a striaght line relationship results. If the choice is too low, the line will deviate upward at longer time points; if the estimate of F_∞ is too high, the line will deviate downward. The longer the time course, the more sensitive are the data to the estimation of F_∞. When ln $[(F_t - F_\infty)/F_t]$ reaches −4, F_t has declined to 2% above F_∞. The slope of the line yields τ, and the intercept of the line at $t = 0$ is ln $[(F_0 - F_\infty)/F_0)$. Figures 7 and 8 show data fit by this procedure. The value of F_∞ that yields the linear replot should correspond to that arrived at from extrapolation to $t = 0$. In some cases it does not, indicating a rapid phase of quenching, usually complete in the first few seconds of the time course. In such cases, the kinetics can be fit, with no change in F_∞, by using F_0 extrapolated. The extent of the rapid phase is obtained from the difference between F_0 measured and F_0 extrapolated. If such a discrepancy is not taken into account, the reconstructed time course will deviate from the actual data as illustrated in Figure 10C. Here the curve in the solid line was calculated for $F_0 = 1$, and the curve in the dashed line was calculated for $F_0 = 1.05$. Thus, if a rapid phase of quench following $t = 0$ reduces the fluorescence (e.g., by 5%) before the quenching of large vesicles proceeds, the initial scaled value of F_0 will be inappropriately large for the bulk of the vesicle population. Such a shift was noted for Figure 7.

The relationships derived here are for an average, ideal, nonleaky vesicle. It should be recalled, however, that the suspension will contain a subpopulation of leaky vesicles that will not participate in electroneutral exchange concentration of Tl^+. These will contribute more weakly to the quench signal and will not be much affected in kinetics of magnitude by activation or blockade of channels. Their contribution may be subtracted before data analysis. Tight vesicles will contribute a fluorescence but will not contribute to the quenching time course unless one or more channels are activated. Thus, it can be easily shown that changes produced in $[(F_0 - F_\infty)/F_0]$ by an activating neurotoxin represents recruitment of otherwise tight vesicles into the quench reaction.

Registry No. Na, 7440-23-5; veratridine, 71-62-5; batrachotoxin, 23509-16-2; tetrodotoxin, 4368-28-9.

References

Agnew, W. S. (1984) *Annu. Rev. Phys. 46*, 517–530.

Agnew, W. S., & Raftery, M. A. (1979) *Biochemistry 18*, 1912–1919.

Agnew, W. S., Levinson, S. R., Brabson, J. S., & Raftery, M. A. (1978) *Proc. Natl. Acad. Sci. U.S.A. 75*, 2606–2610.

Barchi, R. L., Cohen, S. A., & Murphy, L. E. (1980) *Proc. Natl. Acad. Sci. U.S.A. 77*, 1306–1310.

Cahalan, M. (1980) in *The Cell Surface and Neuronal Function* (Cotman, C. W., Poste, G., & Nicolson, G. L., Eds.) pp 1–47, Elsevier/North-Holland Biomedical Press, Amsterdam.

Catterall, W. A. (1977) *J. Biol. Chem. 252*, 8669–8676.

Eftink, M. R., & Ghiron, C. A. (1981) *Anal. Biochem. 114*, 199–227.

Fox, J. M. (1974) *Pflugers Arch. 351*, 287–301.

Garty, H., Rudy, B., & Karlish, S. J. D. (1983) *J. Biol. Chem. 258*, 13094–13099.

Gasko, O. D., Knowles, A. F., Shertzer, H. G., Suolinna, E.-M., & Racker, E. (1976) *Anal. Biochem. 72*, 57–65.

Goldman, D. E. (1943) *J. Gen. Physiol. 27*, 37–60.

Gutknecht, J. (1983) *Biochim. Biophys. Acta 735*, 185–188.

Hanke, W., Boheim, G., Barhanin, J., Pauron, D., & Lazdunski, M. (1984) *EMBO J. 3*, 509–515.

Hartshorne, R. P., & Catterall, W. A. (1981) *Proc. Natl. Acad. Sci. U.S.A. 78*, 4620–4624.

Hartshorne, R. P., & Catterall, W. A. (1984) *J. Biol. Chem. 259*, 1667–1675.

Hartshorne, R. P., Keller, B. U., Talvenheimo, J. A., Catterall, W. A., & Montal, M. (1985) *Proc. Natl. Acad. Sci. U.S.A. 82*, 240–244.

Henderson, R., Ritchie, J. M., & Strichartz, G. R. (1974) *Proc. Natl. Acad. Sci. U.S.A. 71*, 3936–3940.

Hille, B. (1972) *J. Gen. Physiol. 59*, 637–658.

Hodgkin, A. L., & Katz, B. (1949) *J. Physiol. (London) 108*, 37–77.

Huang, L.-Y. M., Catterall, W. A., & Ehrenstein, G. (1979) *J. Gen. Physiol. 73*, 839–854.

Huang, L. M., Moran, N., & Ehrenstein, G. (1984) *Biophys. J. 45*, 313–322.

Khodorov, B. I. (1978) *Membr. Transp. Processes 2*, 153–174.

Krueger, B. K., & Blaustein, M. P. (1980) *J. Gen. Physiol. 76*, 287–313.

Krueger, B. K., Worley, J. F., III, & French, R. J. (1983) *Nature (London) 303*, 172–175.

Levinson, S. R., Curatalo, C. J., Reed, J., & Raftery, M. A. (1979) *Anal. Biochem. 99*, 72–84.

Lombet, A., & Lazdunski, M. (1984) *Eur. J. Biochem. 141*, 651–660.

Miller, C. (1984) *Annu. Rev. Physiol. 46*, 549–558.

Miller, J. A., Agnew, W. S., & Levinson, S. R. (1983) *Biochemistry 22*, 462–470.

Moore, H.-P. H., & Raftery, M. A. (1980) *Proc. Natl. Acad. Sci. U.S.A. 77*, 4509–4513.

Rosenberg, R. L., Tomiko, S. A., & Agnew, W. S. (1984a) *Proc. Natl. Acad. Sci. U.S.A. 81*, 1239–1243.

Rosenberg, R. L., Tomiko, S. A., & Agnew, W. S. (1984b)

Proc. Natl. Acad. Sci. U.S.A. 81, 5594-5598.
Talvenheimo, J. A., Tamkun, M. M., & Catterall, W. A. (1982) *J. Biol. Chem. 257*, 11868-11871.
Tamkun, M. M., & Catterall, W. A. (1981) *Mol. Pharmacol. 19*, 78-86.
Tamkun, M. M., Talvenheimo, J. A., & Catterall, W. A. (1984) *J. Biol. Chem. 259*, 1676-1688.
Tanaka, J. C., Eccleston, J. F., & Barchi, R. L. (1983) *J. Biol. Chem. 258*, 7519-7526.
Tomiko, S. A., Rosenberg, R. L., & Agnew, W. S. (1984) *Soc. Neurosci. Abstr. 10*, 864.
Udenfriend, S. (1962) *Fluorescence Assay in Biology and Medicine*, pp 498-501, Academic, New York.
Ulbricht, W. (1979) *Adv. Cytopharmacol. 3*, 363-371.
Villegas, R., Villegas, G. M., Suarez-Mata, Z., & Rodriguez, F. (1983) *Struct. Funct. Excitable Cells*, [*Int. Conf.*] (Chang, D. C., Tasaki, I., Adelman, W. J., Jr., & Leuchtag, H. R., Eds.) pp 453-469, Plenum, New York.
Weigele, J. B., & Barchi, R. L. (1982) *Proc. Natl. Acad. Sci. U.S.A. 79*, 3651-3655.
Wu, W. C-S., Moore, H.-P. H., & Raftery, M. A. (1981) *Proc. Natl. Acad. Sci. U.S.A. 78*, 775-779.

Fourier-Transform Infrared Studies of CaATPase/Phospholipid Interaction: Survey of Lipid Classes†

G. Anderle and R. Mendelsohn*
Department of Chemistry, Newark College of Arts and Science, Rutgers University, Newark, New Jersey 07102
Received September 19, 1985; Revised Manuscript Received December 9, 1985

ABSTRACT: CaATPase from rabbit skeletal muscle has been isolated, purified, delipidated, and reconstituted with retention of ATPase activity into lipid vesicles consisting respectively of 1,2-dipalmitoylphosphatidylethanolamine, 1-palmitoyl-2-oleoylphosphatidylethanolamine (POPE), 1-stearoyl-2-oleoylphosphatidylcholine (SOPC), and egg sphingomyelin. The effect of the enzyme on phospholipid order and melting characteristics were determined with Fourier-transform infrared spectroscopy. Taken together with prior data from this laboratory for 1,2-dipalmitoylphosphatidylcholine and 1,2-dioleoylphosphatidylcholine (DOPC), as well as for native sarcoplasmic reticulum (SR), three types of lipid response to protein incorporation have been observed: (1) Phospholipids with high levels of acyl chain unsaturation (DOPC or native SR) have their lipid acyl chains slightly ordered by CaATPase incorporation. The effect of protein on the gel–liquid crystal phase transition cannot be easily determined, since the cooperative melting even in these systems occurs at temperatures well below 0 °C. (2) Phospholipids with saturated acyl chains show slightly lowered melting temperatures and reduced cooperativity of melting upon CaATPase insertion. In addition, protein induces (at most) slight disorder into the acyl chains at temperatures removed from the lipid melting point. (3) The strongest response is observed for phospholipids containing one saturated and one unsaturated chain (POPE or SOPC) or heterogeneous systems with low levels of unsaturation (egg sphingomyelin). In these cases, relatively low protein levels diminish the magnitude of or completely abolish the phospholipid phase transition. In addition, substantial disorder is introduced into the acyl chain compared with the pure lipid both above and below its transition temperature. The current data suggest that specific models for lipid/protein interaction based on a single system will not be easily generalized. The interaction between lipid and protein appears to be a strong function of acyl chain unsaturation levels, so that the relative magnitudes of lipid/lipid and lipid/protein interactions, which determine lipid response to protein insertion, become strongly dependent upon both the particular lipids and proteins used.

The well-documented dependence of membrane-bound enzyme activity on the chemical structure or physical state of the phospholipid environment has resulted in many physical studies aimed at elucidation of the molecular basis of lipid/protein interaction [for reviews, see Gennis & Jones (1977) and Parsegian (1982)]. Spectroscopic investigations are generally directed toward determination of changes in the conformation or dynamics of either the lipid or protein component upon their association in reconstituted systems.

To date, the majority of studies involving reconstituted complexes have utilized a small fraction of the available lipid classes, frequently phosphatidylcholines with two saturated acyl chains. Yet this acyl chain distribution is not representative of native membrane environments. In particular, naturally occurring lipids often contain a saturated acyl chain at the *sn*-1 carbon and an unsaturated moiety at the *sn*-2. In addition, native membranes are heterogeneous with regard to lipid head group composition. The purpose of this study is to determine the effect of varying lipid composition (both head group and acyl chain) on protein-induced perturbation of lipid order and thermotropic properties.

The protein chosen for this investigation is CaATPase (ATP phosphohydrolase, EC 3.6.1.3) isolated from rabbit sarcoplasmic reticulum (SR).[1] This protein was selected for two reasons. First, techniques have been developed in several laboratories (Warren et al., 1974a,b; Hidalgo et al., 1976) for replacement of the native SR lipids with a variety of exogenous

† This work was supported by grants to R.M. from the National Institutes of Health (GM 29864) and from the Busch Memorial Fund of Rutgers University.

[1] Abbreviations: SR, sarcoplasmic reticulum; DPPE, 1,2-dipalmitoylphosphatidylethanolamine; POPE, 1-palmitoyl-2-oleoylphosphatidylethanolamine; SOPC, 1-stearoyl-2-oleoylphosphatidylcholine; ESPH, egg sphingomyelin; DPPC, 1,2-dipalmitoylphosphatidylcholine; DOPC, 1,2-dioleoylphosphatidylcholine; FT-IR, Fourier-transform infrared; ESR, electron spin resonance; NMR, nuclear magnetic resonance; Tris, tris(hydroxymethyl)aminomethane.

0006-2960/86/0425-2174$01.50/0